

HiSST: 4th International Conference on High-Speed Vehicle Science Technology

22 -26 September 2025, Tours, France



Two-dimensional numerical analysis of the effect of turbo-ramjet nozzle geometry on scramjet thrust performance in a TBCC engine

Mika Edahiro¹, Akiko Matsuo², Tatsushi Isono³, Masahiro Takahashi⁴, Sadatake Tomioka⁵

Abstract

Turbine-based combined cycle (TBCC) engine represents one of the most promising propulsion technologies capable of sustained hypersonic flight. To achieve optimal thrust generation across the entire flight envelope, it is crucial to optimize the TBCC nozzle geometry, which directly governs both thrust and lift generation. This study examined the influence of direct turbo-ramjet to scramjet flow path integration on the scramjet's propulsive performance at cruising speeds, specifically in the absence of any variable mechanisms such as sliding plates or variable splitter to regulate the flow distribution between the two passages. The computational domain was based on the Single Expansion ramp nozzle (SERN) configuration, employing a scramjet's nozzle inlet height of 163 mm and a length of 3058 mm, while investigating four cases involving cowl to turbo-ramjet flow path distances ranging from 220 mm to 820 mm. The inflow into the nozzle originates exclusively from the scramjet inlet, characterized by a Mach number 1.97, the static pressure of 103.7 kPa, and a static temperature of 2518 K. The two-dimensional compressible Navier-Stokes equation was adopted as the governing equation for the numerical analysis. The result revealed a thrust reduction of 2.3 % for the 820 mm configuration, the case corresponding to the most downstream integration point with the turbo-ramjet flow path, when compared with the baseline SERN configuration.

Keywords: Turbine based combined cycle, Single expansion ramp nozzle, CFD

Nomenclature

Latin

A – Aria, m²

E – Inviscid flux vector in x direction

 $\mathbf{E_v}$ – Viscos flux vector in x direction

e – Total energy, J/m³

F_t - Thrust, N/m

 F_1 – Lift, N/m

F – Inviscid flux vector in y direction

F_v – Viscos flux vector in y direction

h – Specific enthalpy, J/kg

L – Length

M - Mach number

Q – Conserved-quantity vector

T – Temperature, K

t - Time, s

u – Velocity in x direction, m/s

v – Velocity in y direction, m/s

x, y – Coordinate

Greek

 ρ – Density, kg/m³

 τ – Shear stress, Pa

 θ – Angle, degree

Subscripts

i – Chemical species

w - wall

¹ Keio University, 3-14-1 Hiyoshi, Kohoku, Yokohama, mika.edahiro@keio.jp

² Keio University, 3-14-1 Hiyoshi, Kohoku, Yokohama, matsuo@mech.keio.ac.jp

³ Japan Aerospace Exploration Agency, 1 Koganesawa, Kimigaya, kakuda, isono.tatsushi@jaxa.jp

⁴ Japan Aerospace Exploration Agency, 1 Koganesawa, Kimigaya, kakuda, takahashi.masahiro@jaxa.jp

⁵ Japan Aerospace Exploration Agency, 1 Koganesawa, Kimigaya, kakuda, tomioka.sadatake@jaxa.jp

1. Introduction

There is a significant demand for the high-speed transportation of people and materials. High-speed transportation at flight Mach numbers exceeding 5.5 has been identified as having substantial market potential [1]. Airbreathing hypersonic vehicles represent a promising next-generation technology for hypersonic transportation and reusable space launch systems. Recently, in Japan, a new research program on hypersonic transportation has been launched under the Key and Advanced Technology R&D through the Cross-Community Collaboration Program, administered by Japan Science and Technology Agency. This initiative, called the K Program, aims to advance research and development in this field, which is driven by Japan Aerospace Exploration Agency (JAXA) [2][3].

This program aims to demonstrate fundamental technologies for a composite engine system capable of operating across a wide range of flight speeds. To achieve sustained hypersonic flight, a hypersonic vehicle must utilize multiple propulsion systems, each optimized for different speed regimes. One promising approach involves a sequential transition between propulsion systems [4]. At take-off, a turbojet engine provides initial thrust. As the vehicle accelerates to approximately Mach 2, the turbojet engine is deactivated, and a ramjet engine takes over. Beyond Mach 5, the ramjet transitions to a scramjet engine, which enables efficient propulsion at hypersonic speeds. Among the various propulsion system configurations, the turbine-based combined cycle (TBCC) engine is considered the most promising candidate. Fig. 1 illustrates the TBCC engine which is combined turbojet, ramjet and scramjet engines. TBCC engines have garnered significant research interest due to their high specific impulse and broad operational flight envelope, making them well-suited for applications in hypersonic transportation and reusable space launch systems.

Among the component of a combined engine, TBCC exhaust nozzles play a crucial role in generating the majority of thrust for the vehicle. These nozzle's performance significantly affects the propulsion system's overall efficiency. For this reason, the exhaust paths from combined engines must be carefully and efficiently integrated. For instance, TBCC exhaust nozzles primarily operate in cruse conditions with high Mach numbers, utilizing only the scramjet exhaust path. This necessitates incorporation an adjustment mechanism to switch between exhaust paths, such as sliding plates or variable splitter [4][5], which could increase the complexity and weight of the nozzle systems.

One of the primary challenges in the design of TBCC exhaust nozzles lies in achieving high propulsion performance without relying on variable adjustment mechanisms. This study aims to investigate the influence of the connection between the turbo-ramjet and the scramjet flow paths on cruise-point operational efficiency. The scramjet flow path is modelled as a single expansion ramp nozzle (SERN), and a two-dimensional TBCC exhaust nozzle configuration without any flow-adjustment mechanisms is employed for numerical simulations. Initially, under a scramjet cruise condition, a numerical analysis of the flow field structure within the SERN is conducted at the nozzle scale, based on the preliminary design framework of the ongoing K program. Subsequently, variations in the flow field are examined when the turbo-ramjet flow path is integrated above the scramjet flow path as part of the TBCC exhaust system. Finally, the impact on thrust performance is analyzed by altering the axis position of the turbo-ramjet flow path connection relative to the SERN. By quantitatively assessing performance deviations induced by different connection positions, the findings provide critical insights for system-level trade studies, enabling the evaluation of whether flow field regulation via variable mechanisms is necessary. This study establishes a valuable reference for the future design and optimization of TBCC exhaust nozzles and contributes directly to Japan's K Program.

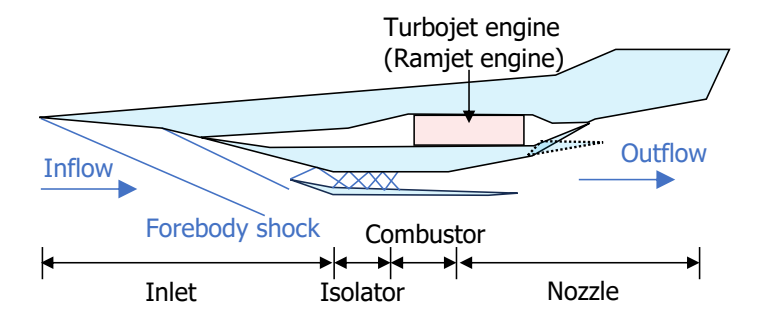


Fig 1. TBCC engine combined turbojet, ramjet and scramjet engines

2. Numerical setup

2.1. Governing equations

In this study, the two-dimensional compressible Navier-Stokes equations shown in Eq. 1 below, the conservation laws for nine chemical species (H_2 , O_2 , N_2 , H_2O , Ar, OH, H, O, NO) and the thermally perfect gas was assumed. In order to close the equation, the ideal gas equation of state is used in Eq. 2. The thermodynamic properties were calculated by NASA polynomials [6]. For the discretization of the convective terms, the Yee's non MUSCL type2nd-order TVD upwind scheme [7] was employed. Time integration was performed using the LU-ADI implicit method [8][9]. The $k-\omega$ model for RANS [10] was also used as the turbulence model.

$$\frac{\partial \hat{\mathbf{Q}}}{\partial t} + \frac{\partial (\hat{\mathbf{E}} - \hat{\mathbf{E}}_{\mathbf{v}})}{\partial \xi} + \frac{\partial (\hat{\mathbf{F}} - \hat{\mathbf{F}}_{\mathbf{v}})}{\partial \eta} = \mathbf{0} \tag{1}$$

$$\hat{\mathbf{Q}} = \frac{1}{J} \begin{bmatrix} \rho \\ \rho u \\ \rho v \\ \rho i \end{bmatrix}, \hat{\mathbf{E}} = \frac{1}{J} \begin{bmatrix} \rho U \\ p\xi_x + \rho uU \\ p\xi_y + \rho vU \\ (e+p)U \\ \rho_i U \end{bmatrix}, \hat{\mathbf{F}} = \frac{1}{J} \begin{bmatrix} \rho V \\ p\eta_x + \rho uV \\ p\eta_y + \rho vV \\ (e+p)V \\ \rho_i V \end{bmatrix}$$

$$\hat{\mathbf{E}}_{\mathbf{v}} = \frac{1}{J} \begin{bmatrix} 0 \\ \xi_x \tau_{xx} + \xi_y \tau_{xy} \\ \xi_x \tau_{xx} + \xi_y \tau_{yy} \\ \xi_x \beta_x + \xi_y \beta_y \\ \xi_x \rho D_i \frac{\partial Y_i}{\partial x} + \xi_y \rho D_i \frac{\partial Y_i}{\partial y} \end{bmatrix}, \hat{\mathbf{F}}_{\mathbf{v}} = \frac{1}{J} \begin{bmatrix} 0 \\ \eta_x \tau_{xx} + \eta_y \tau_{xy} \\ \eta_x \tau_{yx} + \eta_y \tau_{yy} \\ \eta_x \beta_x + \eta_y \beta_y \\ \eta_x \rho D_i \frac{\partial Y_i}{\partial x} + \eta_y \rho D_i \frac{\partial Y_i}{\partial y} \end{bmatrix}$$

$$p = \sum_i \rho_i R_i T$$
(2)

2.2. Calculation targets

This study analyzed the operational characteristics of scramjet engine under the combustion gas conditions, where a flow with a Mach number of 1.97, a static pressure of 103.7 kPa, and a static temperature of 2518 K was introduced through the scramjet nozzle inlet. These parameters correspond to a fight Mach number of approximately 6.0, as assumed in a previous collaborative study with JAXA. The thermodynamic properties of the combustion gas and external airflow are summarized in Table 1, while the mole fraction of the combustion gas, based on hydrogen-fueled combustion, is presented in Table 2.

The nozzle geometry was based on a SERN configuration. The computational domain is defined with an inlet height of 163mm, an outlet height of 1276 mm, a nozzle length of 3058 mm, and a cowl length of 156 mm (approximately 5% of the nozzle length). The initial expansion angle of the scramjet nozzle inlet, corresponding to the ramp wall angle, was set to 20 degrees. To configure the model as a TBCC nozzle, a 311 mm-wide turbo-ramjet flow path was integrated along the ramp surface of the SERN, resulting in a rear ramp angle of 14 degrees.

For the scramjet operating mode, it is assumed that the turbo-ramjet system is inactive, with its inlet fully closed and no airflow within the turbo-ramjet passage. Based on this concept, the study evaluates whether the exhaust-side flow path should be sealed at specific locations to optimize performance.

Table 1. Combustion gas and External air conditions introduced through the nozzle inlet

Type of inflow	Mach number [-]	Pressure [kPa]	Temperature [K]
Combustion gas	1.97	103.7	2518.3
External air	6.86	2.97	300

Table 2. Mole fraction rate of the combustion gas (at Mach number 1.97)

H ₂	02	N_2	H ₂ O	Ar	ОН	Н	0	NO
0.0419	0.0190	0.627	0.288	0.00755	0.00819	0.000555	0.00691	0.00214

Consequently, the computational domain was designed to assess the influence of closing the rear connection point of the turbo-ramjet flow path during the initial stage of analysis, as illustrated in Fig. 2. The grid size near the wall was 10 μ m with a minimum y^+ of 0.1. The inner nozzle surface was treated as an isothermal, no-slip wall, while the nozzle outlet boundary condition was defined using an extrapolation method.

Subsequently, the influence of the turbo-ramjet connection position on scramjet engine's performance was investigated. The connection point of turbo-ramjet was modified as illustrated in Fig. 3. Four computational cases ware conducted, as summarized in Table 3. The vertical distance between the turbo-ramjet flow path and the scramjet cowl \boldsymbol{L} has been increased from 220 mm to 820 mm, while the rear ramp wall angle $\boldsymbol{\theta}$ decreased from 14.0 degrees to 5.7 degrees accordingly.

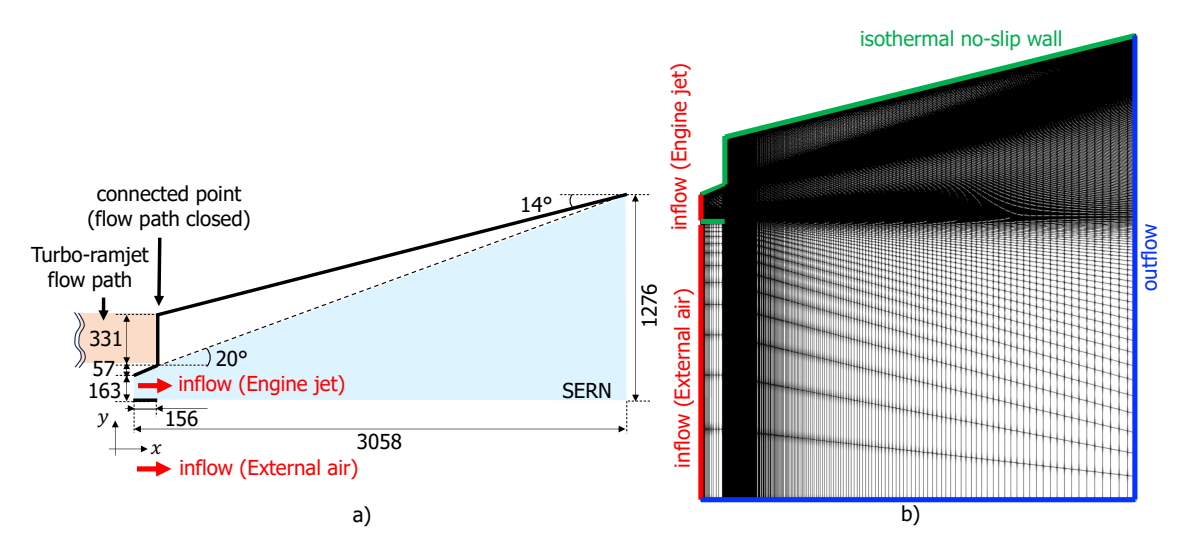


Fig 2. Calculation domain and boundary condition in TBCC nozzle and SERN comparison: a) calculation domain and b) boundary condition

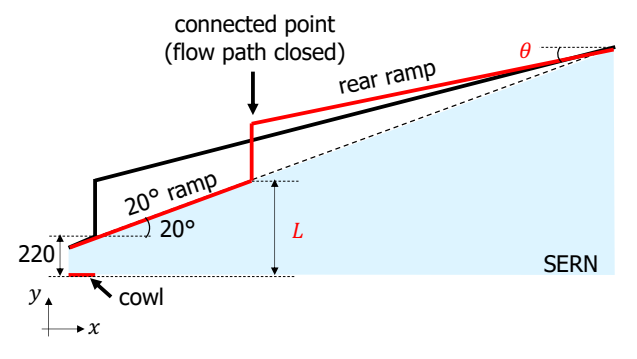


Fig 3. Calculation domain in the turbo-ramjet connection point investigation

Table 3. The distance between the two flow paths and corresponding rear ramp angle

case number	Distance between the two flow paths L [mm]	Angle of the rear ramp wall θ [deg]
case_220	220	14.0
case_420	420	12.6
case_620	620	10.2
case_820	820	5.7

3. Results and discussion

3.1. Influence of turbo-ramjet exhaust coupling on scramjet performance

In addition to the TBCC nozzle including with the turbo-ramjet exhaust port, SERN with a 5% cowl length (highlighted in blue in Fig. 2) was analyzed for the comparative assessment. The internal thrust and lift forces were calculated from the wall pressure using Eq. 3 and Eq. 4.

$$F_t = \int p_w dA_{w,t} - \int \tau_w dA_{w,t} \tag{3}$$

$$F_l = \int p_w dA_{w,l} - \int \tau_w dA_{w,l} \tag{4}$$

Fig. 4 presents the pressure, Mach number, and temperature distributions of SERN configuration. While the Fig. 5 shows the corresponding distributions for the TBCC nozzle. In both configurations, the combustion gases entering from the scramjet nozzle inlet expanded along the 20 degrees scramjet ramp surface. In the TBCC nozzle, the flow was forcefully expanded from the ramp tip toward the 14 degrees rear ramp, generating an oblique shock wave that propagated downstream from the point of interaction with the rear ramp surface. Fig. 6 represents the pressure rate distribution along the ramp surface, nondimensionalized by the scramjet nozzle inlet pressure. The primary flow detached from the trailing edge of the front ramp and subsequently reattached to the rear ramp, generating a shock wave and inducing a pressure rise. Moreover, the primary flow expanded rapidly at the trailing edge of the front ramp, resulting in a localized pressure reduction which further contributed to a pressure decrease within the back step region. A recirculating vortex developed inside the back step and its velocity was considerably lower than that of the main flow, thereby leading to a localized temperature increase within the region.

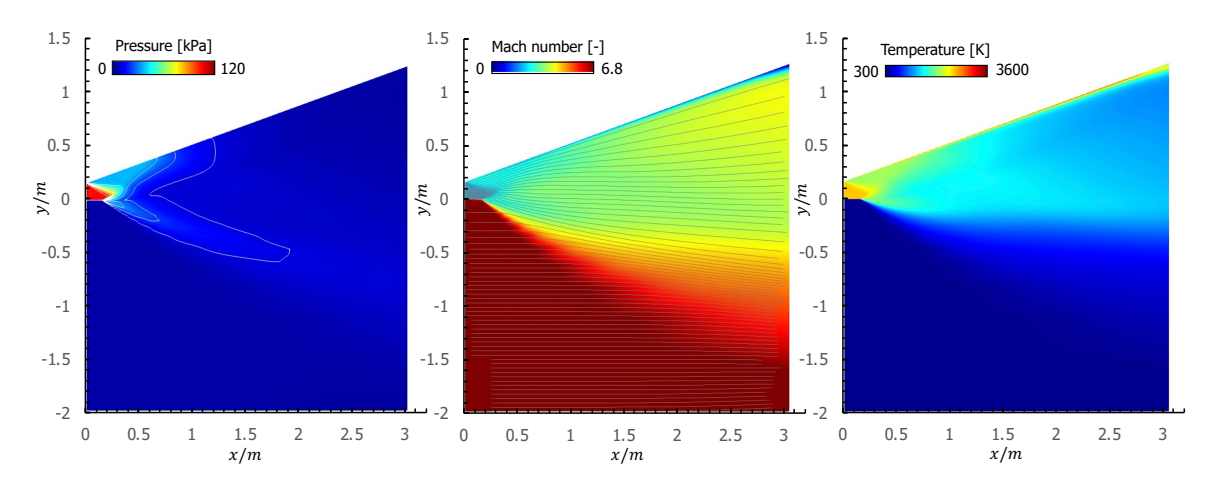


Fig 4. The pressure, Mach number and temperature distribution of SERN

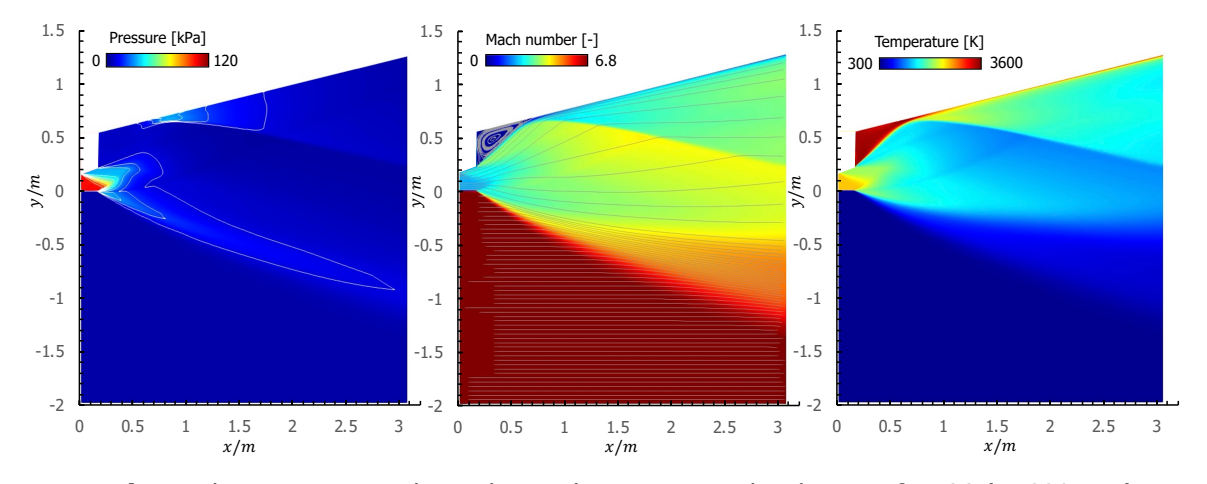


Fig 5. The pressure, Mach number and temperature distribution of TBCC (L=220 mm)

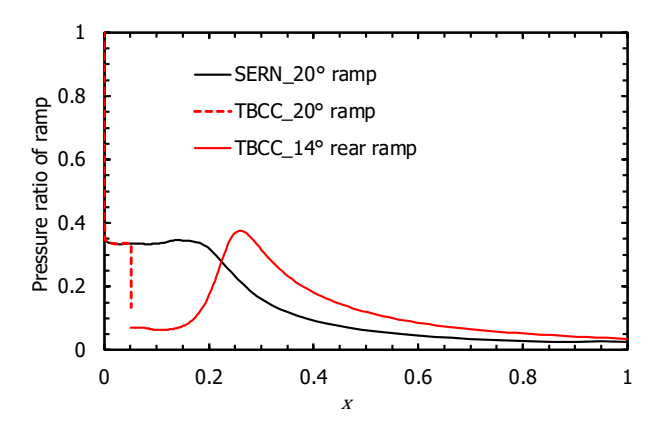


Fig 6. Pressure distribution of ramp surface (the pressure was divided by the scramjet inlet pressure, x was divided nozzle length)

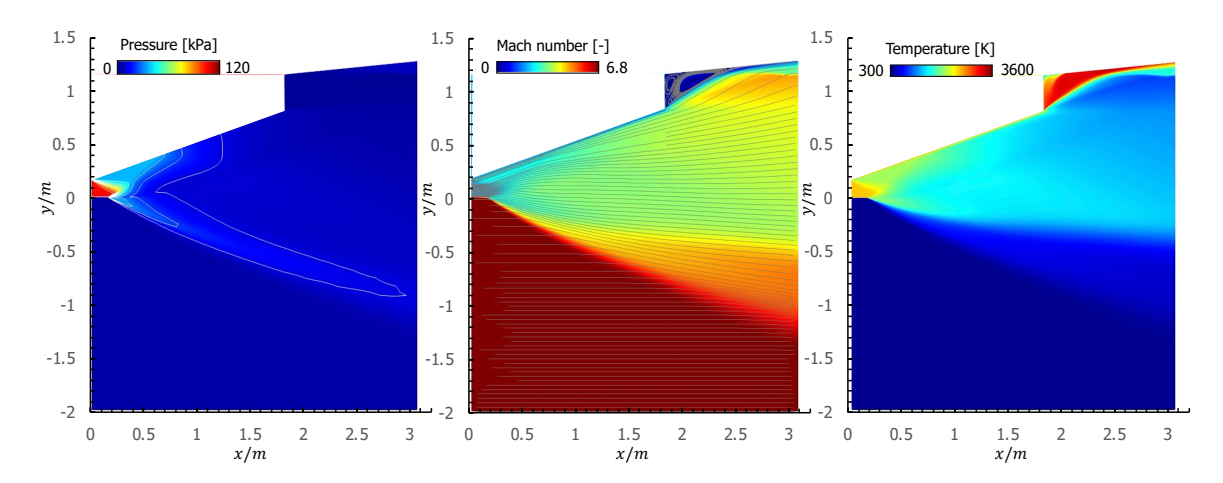


Fig 7. The pressure, Mach number and temperature distribution (L=820 mm)

This temperature rises requires careful evaluation, as it may influence the decision on whether the downstream turbo-ramjet duct should be closed during scramjet operation. The computed internal thrust values for the two configurations were 12.9 kN/m for the TBCC nozzle and 14.1 kN/m for the SERN, corresponding to an approximate 9% thrust reduction in TBCC configuration. This loss in thrust was primarily attributed to the localized pressure deficit formed near the turbo-ramjet connection port.

3.2. Influence of Turbo-ramjet coupling position on scramjet performance

In the next stage, the effect of varying the Turbo-ramjet coupling position, as specified in Table 3, was investigated to evaluate its impact on overall performance. Fig. 7 shows the pressure, Mach number, and temperature distributions for the TBCC nozzle in case_820. The flow characteristics upstream of the turbo-ramjet coupling closely resembled those observed for the SERN configuration in Fig. 4. Beyond this point, the main flow was directed toward the upper wall but at a shallower inclination compared to case 220 in Fig. 5. After the main flow collided with the upper wall of the turbo-ramiet flow path, main stream generated an oblique shock wave downstream of the interaction region, while a significant pressure reduction was observed near the coupling interface. Fig. 8 shows the pressure ratio distributions along the ramp surface for all configurations listed in Table 3. The pressure profile on the 20 degrees ramp surface exhibited a similar trend to that of the SERN in Fig. 6. Initially, a noticeable pressure reduction was observed at the onset of flow expansion, followed by a sharp pressure drop near the turbo-ramjet coupling point. However, as the connection point was positioned further downstream, the main flow approached the trailing edge of the front ramp in a more fully expanded state, resulting in a relatively lower pressure drop rate within the back step region. After that the main flow collided with the aft ramp surface, inducing a localized pressure increase. Nevertheless, the magnitude of this rise diminished progressively with downstream displacement of the junction. Subsequently, the flow underwent gradual expansion along the rear ramp.

The computed thrust and lift results for all cases are summarized in Fig. 9 and Table 4. For case_820, the thrust was calculated to be 13.8kN/m, representing a marginal decrease of approximately 2.3 % compared to the SERN configuration. This suggests that the pressure reduction induced by the back step exerts only a minor influence on thrust diminution when the flow expansion is already sufficiently developed at the coupling interface with the turbo-ramjet flow path. On the other hand, the lift forces in all cases represented similar values. There findings indicate that, to minimize thrust losses relative to the SERN configuration, it is advantageous to position the turbo-ramjet coupling downstream of the ramp region. Furthermore, a comprehensive trade-off analysis is required to evaluate the relationship between thrust reduction and the potential weight penalties associated with integrating additional actuation mechanisms. In parallel, a detailed investigation of the thermal effects near the turbo-ramjet connection interface is necessary to ensure structural integrity and operational reliability under scramjet operating conditions.

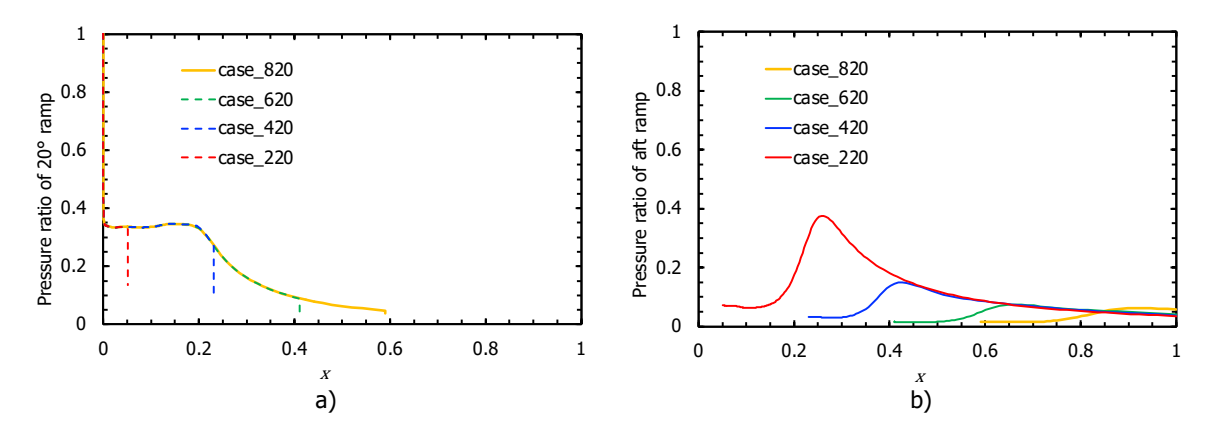


Fig 8. Pressure distribution of ramp surface: a) 20 degrees from ramp and b) aft ramp, the pressure was divided by the scramjet inlet pressure, x was divided by nozzle length

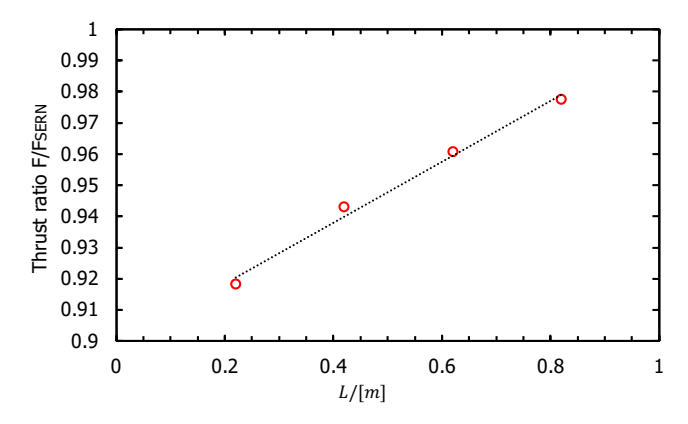


Fig 9. Thrust ratio of TBCC nozzle by the SERN thrust value (*L* has been increased from 220 mm to 820 mm)

Table 4. Summarize of thrust and lift forces of SERN and TBCC nozzle with four cases of L

case number of TBCC nozzle	Thrust [kN/m]	Lift [kN/m]
(Base) SERN	14.1	25.0
case_220	12.9	25.6
case_420	13.3	25.9
case_620	13.5	25.9
case_820	13.8	25.6

4. Conclusion

This study investigated the impact of direct turbo-ramjet integration into the scramjet flow path on the scramjet's propulsive performance at cruising conditions, specifically under configurations without variable mechanisms for regulating flow distribution between the two passages. The computational domain was based on the Single Expansion ramp nozzle (SERN) configuration, employing a scramjet's nozzle inlet height of 163 mm and a length of 3058 mm, while investigating four cases involving cowl to turbo-ramjet flow path distances ranging from 220 mm to 820 mm. The inflow into the nozzle originates exclusively from the scramjet nozzle inlet, characterized by a Mach number 1.97, the static pressure of 103.7 kPa, and a static temperature of 2518 K. The two-dimensional compressible Navier-Stokes equation was adopted as the governing equation for the numerical analysis.

For the forward 20 degrees ramp, the flow characteristics closely matched those of the baseline SERN configuration, exhibiting a gradual pressure decay as the expansion waves originating from the cowl tip propagated toward the ramp surface. This region contributed significantly to the generation of both thrust and lift forces. However, downstream of the turbo-ramjet connection point, the flow behavior within the TBCC nozzle configuration exhibited notable deviations. After the main flow impinged on the rear ramp surface of the turbo-ramjet flow path, an oblique shock wave formed downstream of the interaction zone, accompanied by a substantial pressure deficit near the coupling interface. This localized pressure deficit formed near the turbo-ramjet connection port leaded to the thrust losses.

Parametric analysis revealed that varying the position of the turboramjet connection port along the SERN ramp surface resulted in a thrust reduction rates ranging from 2.3% to 9 %. The smallest thrust loss was observed when the connection port was located furthest downstream, indicating that aft placement of the integration point was advantageous for minimizing performance penalties. In contrast, the lift forces across all configurations exhibited negligible variation.

Overall, the findings indicate that the downstream positioning of the turbo-ramjet coupling can mitigate thrust degradation while maintaining comparable lift performance relative to the Vaseline SERN configuration. Nevertheless, further investigations are warranted to perform a detailed trade-off analysis between thrust efficiency and potential weight penalties associated with incorporating additional actuation mechanisms. Additionally, a detailed investigation of the thermal effects near the turbo-ramjet connection interface is necessary to ensure structural integrity and operational reliability under scramjet operating conditions.

5. Acknowledgment

This work was supported by JST K Program Grant Number JPMJKP23E1, Japan.

References

- 1. Deloitte consulting LPP.: Commercial Hypersonic Transportation Market Study. NASA Technical Reports Server. https://ntrs.nasa.gov/citations/20210014711. Accessed 1 August 2025
- 2. 富岡定毅, 竹腰正雄, 髙橋政浩, 田口秀之, 佐藤哲也, 中谷辰爾, 松尾亜紀子, 笠原次郎, 早川晃弘.: 研究計画「幅広い作動域を有するエンジン設計技術の地上実証」について, 第68回宇宙科学技術連合講演会, 2024 (Sadatake Tomioka, Masao Takegoshi, Masahiro Takahashi, Hideyuki Taguchi, Tetsuya Sato, Shinji Nakaya, Akiko Matsuo, Jiro Kasahara, Akihiro Hayakawa.: On Research Plan Titled as Ground Test Validation of Engine Design Method with Wide Operation Range. 68th Space Sciences and Technology conference (2024)(in Japanede))
- 3. 竹腰正雄, 富岡定毅, 髙橋政浩, 田口秀之, 今村俊介, 高橋俊: 研究計画「幅広い作動域を有するエンジン設計技術の地上実証」の紹介と2024年の進捗について、日本航空宇宙学会北部支部2025年講演会、2025 (Masao Takegoshi, Sadatake Tomioka, Masahiro Takahashi, Hideyuki Taguchi, Shunsuke Imamura, Shun Takahashi.: Introduction of Research Plan Titled as "Ground Test Validation of Engine Design Method with Wide Operation Range" and Progress in 2024. The Japan Society of Aeronautical and Space Sciences Northern Branch conference (2025)(in Japanese))

- 4. Zheng Lv, Jinglei Xu, Guangtao Song, Rui Li, Jianhui Ge.: Review on the aerodynamic issues of the exhaust system for scramjet and turbine based combined cycle engine. Progress in Aerospace Sciences 143 (2023). https://doi.org/10.1016/j.paerosci.2023.100956
- 5. H. Yang, Q. Yang, Z. Mu, Y. Shi, L. Chen, V., Mar.: Effect of a Secondary Injection on the Performance of Three-Dimensional Over-under TBCC Exhaust Nozzles. Journal of Applied Fluid Mechanics (2023). https://doi.org/10.47176/jafm.16.04.1586
- 6. B. J. McBride, S. Corden, M. A. Reno.: Coefficients for Calculating Thermodynamic and Transport Properties of Individual Species. NASA Technical Memorandum 4513 (1993)
- 7. H. C. Yee.: Upwind and Symmetric Shock Capturing Schemes. NASA Technical Memorandum No.89464 (1987)
- 8. S. Obayashi, et al.: Improvements in Efficiency and Reliability for Navier-Stokes Computations Using the Lu-ADI Factorization Algorithm. AIAA 24th Aerospace Sciences Meeting (1986)
- 9. S. Obayashi, et al.: An Approximate LU Factorization Method for the Compressive Navier-Stokes Equations. Journal of Computational Physics, Vol.63 (1986)
- 10. Wilcox, D.C.: Turbulence Modelling for CFD, DCW Industries (2006)